*Nordic Hydrology*, 21, 1990, 165-184



# Rain-Runoff Parameters for Six Small Gauged Urban Catchments

**Mogens Jensen**

Dept. of Environmental Engineering,
Technical University of Denmark, Lyngby

The interpretation of rain-runoff measurements from 6 small (less than 17 ha) urban catchments is described. The recording period covers mostly 1979-1983. Relations between rain- and runoff depths were developed using the traditional linear regression model as well as a new continuous model. Both models compute runoff from impervious surfaces in the same way. Calculation of runoff from semipervious surfaces accounts for infiltration through cracks, percolation from a sublayer and evaporation during dry weather. These phenomena are related to water content of the sublayer. The 10 parameters in the continuous model are calibrated and show values in good agreement with data from the literature. The continuous model fits the measured runoff depths somewhat better for the largest runoff events. For more frequent events, however, the two models are equally good.

Rain intensity – duration – frequency curves have been computed. Variations of up to 20 %, for return periods 1/5 and 1/2 yr., are seen for catchments with distances approximately 5 km from each other.

Peak flow statistics are compared with rain intensity. The peak runoff coefficient (*cf.* rational method) is mostly constant or slightly increasing with the return period.

## Background and Purpose

Since 1974 several research projects within urban drainage have been carried out by the Dept. of Environmental Engineering, Technical University of Denmark, with financial support from several public organisations.

A central part of these research efforts has been to determinate parameters for urban catchments necessary for the transformation of rainfall to runoff. In this respect 6 small study catchments have been selected and equipped with automatic rain-runoff gauges. The catchments of Cedervænget (CV), Munkerisparken (MP) and Vestre Paradisvej (VP) were established as reported in Johansen (1985) and Johansen *et al.* (1978-1981). The catchments in Emdrup Banke (EB) and Nannasgade-Vølundsgade (NV) was established as reported in Larsen (1979) and Bispeengsbuen (BB), was etablished for the study of rain-runoff from highways (Statens Vejlaboratorium 1984).

This paper presents the methods used in the data interpretation with respect to rain and runoff statistics, and in the determination of hydrological parameters for impervious and semipervious areas. These methods were essentially the same for all six catchments.

## Catchment Data and Extent of Measurements

Main catchment data appear in Table 1. The division of areas into pavement categories are as follows:

$F_1$ = impervious: Roofs, asphaltic roads, concrete without visible cracks.
$F_2$ = semipervious: Flagstones, paving stones, firm gravel pavement and concrete with visible cracks.
$F_3$ = pervious: All unpaved areas.

The full-flow travel time $t_f$ is the sum of pipelength divided by full-flow velocity (Manning formula). The branch with the largest $t_f$-value (*cf.* time-area model) is used.

Table 1 – Main catchment data. ($F$ ≡ total area; $F_1$ ≡ impevious area; $F_2$ ≡ semipervious area; $F_3$ ≡ pervious area; Com. ≡ combined; Sep. ≡ separate; $t_f$ = full-flow travel time for sewer system)

| Catch-ment | $F$ (ha) | Areas $F_1$ + $F_2$ + $F_3$ (%) | Sewer System type | $t_f$ (min.) | Latest Reference |
|---|---|---|---|---|---|
| CV | 5.28 | 22 + 23 + 55 | Com. | 4.7 | Jensen *et al.* (1985) |
| MP | 6.44 | 31 + 14 + 54 | Sep. | 9.2 | Jensen *et al.* (1985) |
| VP | 17.15 | 16 + 7 + 77 | Com. | 12.4 | Jensen *et al.* (1985) |
| EB | 4.42 | 47 + 10 + 43 | Com. | 4.7 | Hansen and Kildebro (1985) |
| NV | 1.46 | 78 + 21 + 1 | Com. | 2.2 | Hansen and Kildebro (1985) |
| BB | 1.94 | 78 + 11 + 11 | Sep. | 3.8 | Statens Vejlaboratorium (1984) |

Table 2 – Extent and efficiency of rain (*RA*) – and runoff (*RO*) measurements, including overlaps (*RA* + *RO*)

| Catch-ment | | Extent From-to | Extent Days | Efficiency Days | Efficiency (%) |
|---|---|---|---|---|---|
| | *RA* | 790803-830927 | 1,513.5 | 1,504.5 | 99 |
| CV | *RO* | 790505-830907 | 1,583.5 | 1,444.0 | 91 |
| | *RA*+*RO* | 790803-830907 | 1.493.5 | 1,368.5 | 92 |
| | *RA* | 790601-831004 | 1,583.3 | 1,568.5 | 91 |
| MP | *RO* | 790608-831004 | 1,576.3 | 1,398.8 | 89 |
| | *RA*+*RO* | 790608-831004 | 1,576.3 | 1,395.6 | 89 |
| | *RA* | 790802-831004 | 1,521.3 | 1,476.8 | 97 |
| VP | *RO* | 790806-830901 | 1,483.5 | 1,383.5 | 93 |
| | *RA*+*RO* | 790806-830901 | 1,483.5 | 1,347.3 | 91 |
| | *RA* | 790108-831231 | 1,817.8 | 1,709.0 | 94 |
| EB | *RO* | 790306-830916 | 1,646.1 | 1,531.0 | 93 |
| | *RA*+*RO* | 790306-830916 | 1,646.1 | 1,484.0 | 90 |
| | *RA* | 790124-831231 | 1,800.3 | 1,770.8 | 98 |
| NV | *RO* | 790410-831231 | 1,725.0 | 1,402.8 | 81 |
| | *RA*+*RO* | 790410-831231 | 1,724.3 | 1,400.0 | 81 |
| | *RA* | 730801-821018 | 3,366.0 | 2,034.0 | 60 |
| BB | *RO* | 730801-821018 | 3,366.0 | 1,969.0 | 58 |
| | *RA*+*RO* | 730801-821018 | 3,366.0 | 1,969.0 | 58 |

Extent and efficiency of measurements appear in Table 2. Efficiency of rain measurements (RA) is generally very high. For runoff (RO) efficiency is somewhat lower due to malfunctioning and periodical cleaning of the Palmer-Bowlus or Venturi flumes for deposits.

## Separation of Dry Weather Flow

For all catchments, except BB, dry weather flow was observed. This flow must be subtracted for each single rain-runoff event. An estimate for the dry weather flow and its temporal distribution was derived by using the measured flows within all dry weather periods defined as follows:

A dry weather period begins 24 h after the last tipping of the rain gauge and must have an extension of at least 24 h, with no tippings, to be included in the dry weather flow model.

A flow variation on a weekly basis (168 numbers, one mean value for each hour during a week) was computed. An example of the variation for catchment CV is

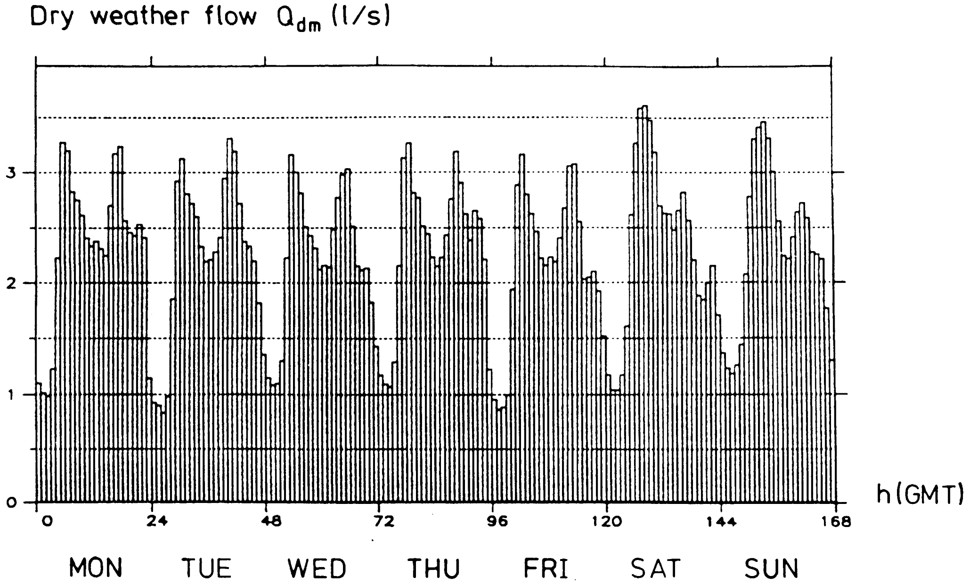


Fig. 1. Computed mean dry weather flow on a weekly basis for CV.

seen in Fig. 1. The weekly basis is better than a daily basis for the computation of runoff from rain, because the temporal pattern as seen in Fig. 1 is different for a working day compared with a weekend day.

This weekly flow was computed for the 4 catchments with combined systems. for MP the flow was found to be small and almost constant 0.3 l/s.

Since the dry weather flow, $Q_d(t)$ during a specific rain-runoff event may vary slightly from the mean distribution $Q_{dm}(t)$ described above, $Q_d(t)$ is computed as

$$Q_d(t) = Q_{dm}(t) + (Q_{do} - Q_{dm}(0)) \tag{1}$$

where $t \equiv 0$ at the beginning of the rain event. $Q_{do}$ is the measured flow at $t = 0$ and $Q_{do} - Q_{dm}(0)$ is thus a simple parallel displacement ($> 0$ or $< 0$).

A reliable estimate of dry weather flow is especially important for the computation of runoff volume from the smaller rains, which appear frequently, and thus have a significant influence on the water balance computation and hydrologic parameters.

## Block Rain – and Peak Flow Statistics

A rain-runoff event begins when the time interval between two tippings of the rain bucket is less than one hour. This corresponds to rain intensity $> 0.2$ mm/h $= 0.056$ $\mu$m/s. Zero time is taken as the time of the first tipping. The event continues until either 1) the time interval above exceeds one hour or 2) the measured discharge is less than the dry weather flow $Q_d$, Eq. (1), plus the standard deviation of $Q_{dm}$.

This procedure transforms the complete time series into a series of single events with known temporal distribution of rain and runoff (time step is 1 min). These series are the basis for derivation of intensity – duration – frequency curves (IDF) for block rain and for computation of peak flow statistics.

IDF-curves describes the frequency $n_a = n_a(i, t_r)$ as a function of the mean rainfall intensity (block rain intensity), $i$, within a selected duration $t_r$. The frequency is identical to the average number of times per year by which the intensity $i$ is exceeded. All rainfalls are considered as independent events so that each rainfall with intensity greater than $i$ (for selected $t_r$) contribute to $n_a$. This statistical principle is named partial duration series (or peak over threshold, POT) and it has been used in Denmark (and many other countries) as the standard for derivation of IDF-curves. It may be noticed that the variation of $n_a(i, t_r)$ is within the interval $n_a(\infty, t_r) \equiv 0 < n_a(i, t_r) < n_a(0,0) \equiv$ average number of rainfalls pr. year. (If the principle of annual peak statistics was used, the upper limit of $n_a$ would be 1).

The procedure for calculating $n_a(i, t_r)$ assumes that it is sufficiently accurate to compute the frequency $n_j(i, t_r)$ for each month, $j$, of the year, and then afterwards add 12 $n_j$-values, hereby achieving

$$n_a(i, t_r) = \frac{1}{T(i, t_r)} \equiv \sum_{j=1}^{12} n_j(i, t_r) \tag{2}$$

where $T(i, t_r)$ is the return period.

Calculation of $n_j(i, t_r)$ takes place as follows:

1) Compute $N_j$ as the equivalent number of effective years of registration for month $j$ ($N_j$ = (number of days with registration) / (calendar days)). $N_j$ is needed since the time series do not cover an integer number of years, and due to occasional malfunctioning of the gauges.
2) Select a value of $t_r$. The actual list was

$$t_r = 5, 10, 20, \cdots, 5{,}120\text{min (increasing by factor of 2)} \tag{3}$$

   Produce 12 tables ($j$ = 1,2 ...12), which list all rain intensities $i$ in decreasing order corresponding to rank $M_j(i, t_r)$.
3) Make a log-linear interpolation in each table, corresponding to a given intensity $i$, and calculate the (non-integer) rank $M_j(i, t_r)$ and the frequency

$$n_j(i, t_r) = \frac{M_j(i, t_r)}{N_j} \tag{4}$$

   by which $i$ is exceeded, within month $j$. By keeping $i$ at a fixed threshold, Eq. (4) is used for all 12 months and the annual frequency $n_a(i, t_r)$, from the complete time series is then given by Eq. (2).

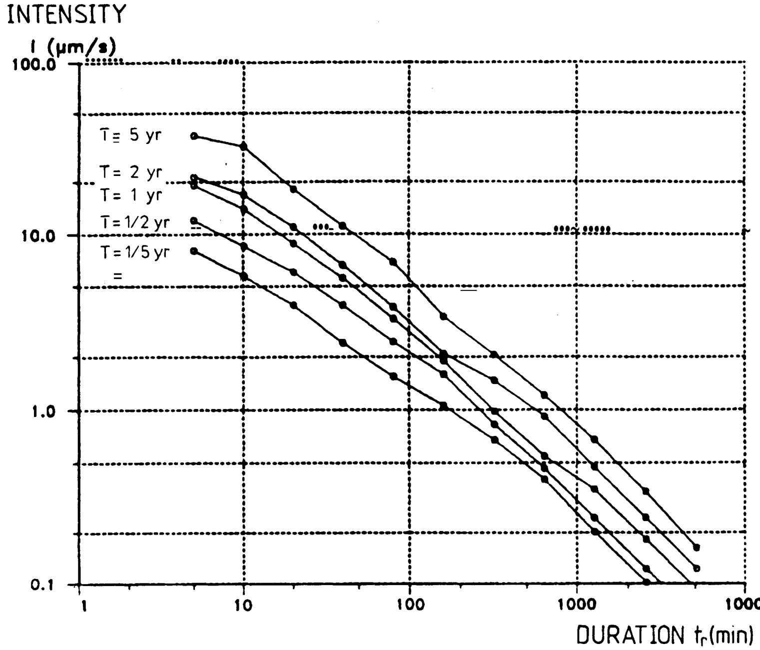


Fig. 2. Intensity-duration-frequency (IDF) curves for CV.

Eq. (4) is called the California formula. The application of this formula is in accordance with Danish tradition, when IDF-curves are of concern. Alternative formulas such as Weibull $n = M/(N+1)$, Hazen $n = (2M\text{-}1)/2N$, etc. are discussed in several hydrology textbooks.

As an example Fig. 2 shows the IDF-curves for CV. For all 6 catchments there were variations with small curvature in a log-log diagram. It must be noted that IDF-curves have increasing inaccuracy with increasing $T$, due to the limited observation period, see Table 2.

Comparisons among the IDF-curves from the 6 catchments appear in Table 3. The logarithmic mean is used

$$i_m = (i_5 \times i_{10} \times i_{20} \times i_{40})^{\frac{1}{4}} \tag{5}$$

relative to $i_m$ for the rain series 1933-72 (40 yr.) from Gentofte (GE), a suburb just north of Copenhagen.

The 5 first catchments in Table 3, for which observation periods are almost identical, show variations up to approximately 20% between the IDF-curves for return periods 1/5 and 1/2 yr. The distance between any two of the catchments is less than 15 km. These variations are considered mainly as spatial variability and not only a consequence of the approximately 4 yr. period of record.

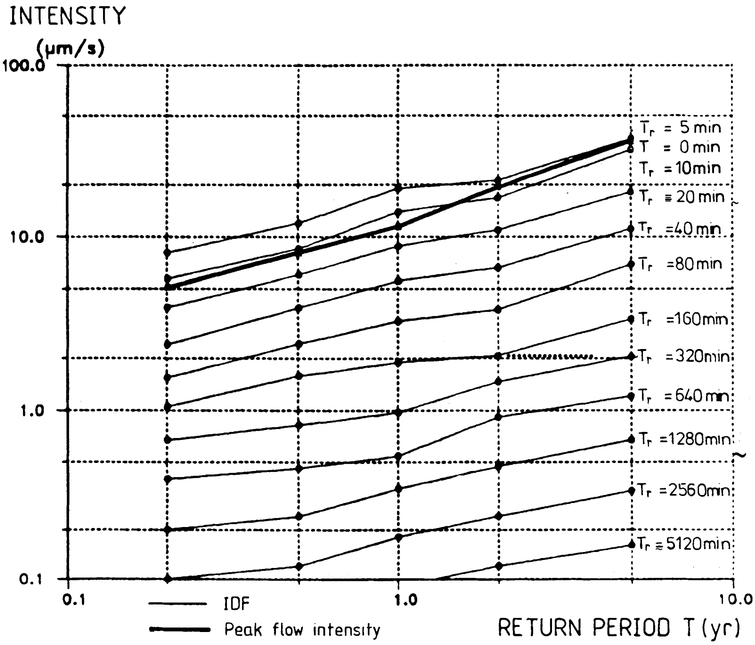


Fig. 3. Peak flow statistics and IDF-curves for CV. Full flow travel time $t_f$ = 4.7 min. for pipes.

Peak flow statistics were derived by computing $Q/(F_1 + F_2)$ = peak discharge/ paved area for each runoff event (duration = timestep = 1 min). Ranking and statistical computations for this quantity was done using Eqs. (4) and (2). As an example Fig. 3 shows the peak flow intensity as function of $T$ for CV and compares this curve with the IDF-curves shown for constant $t_r$-values. As can be seen, peak flow intensity increases a little more with $T$ than does rain intensity. To explain this phenomenon one can compare with the design formula from the rational method

Table 3 – Logaritmic mean $i_m \equiv (i_5 \times i_{10} \times i_{20} \times i_{40})^{1/4}$ (suffix ≡ duration in min.) for the 6 catchments relative to $i_m$ (GE) for Gentofte based on a 40 yr. record 1933-1972

| Return Period $T$ (yr.) | 1/5 | 1/2 | 1 | 2 |
|---|---|---|---|---|
| $i_m$ (GE) (μm/s) | 3.75 | 5.90 | 7.64 | 9.76 |
| $i_m$ (CV)/$i_m$ (GE) | 1.22 | 1.18 | 1.39 | 1.30 |
| $i_m$ (MP)/$i_m$ (GE) | 1.09 | 1.00 | 0.97 | 0.91 |
| $i_m$ (VP)/$i_m$ (GE) | 1.05 | 0.95 | 0.88 | 0.75 |
| $i_m$ (EB)/$i_m$ (GE) | 1.00 | 1.00 | 1.01 | 0.96 |
| $i_m$ (NV)/$i_m$ (GE) | 1.21 | 1.17 | 1.09 | 0.92 |
| $i_m$ (BB)/$i_m$ (GE) | 1.00 | 0.90 | 0.88 | 0.83 |

$$\frac{Q}{(F_1+F_2)}=\Phi_p i(t_c) \qquad (6)$$

where $\phi_p$ is a peak runoff coefficient and $i(t_c)$ is the design rain intensity, corresponding to a time of concentration $t_c$. Rainfall intensities will increase with increasing $T$, and $\phi_p$ is also expected to increase slightly due to a more or less constant loss intensity from hydrological phenomena (infiltration, *etc.*) For increasing rain intensities, $t_c$ will decrease, due to a more rapid response from overland flow and consequently also $i(t_c)$ is expected to increase with $T$.

The steeper slope of the $Q/(F_1 + F_2)$-curve, compared with the slope of the IDF-curve, appears clearly for CV and VP. For MP, EB and NV, the two curves were almost parallel. For BB the slope of $Q/(F_1 + F_2)$ was less than the slope of rain intensity. This deviation from expected behaviour for BB has not been explained with certainty.

## Linear Regression inbetween Rain – and Runoff Depths

One of the standard methods in the study of rain – runoff depths relations is to carry out a linear regression

$$\frac{V}{(F_1+F_2)} \equiv \Phi(R-S) \; ; \quad \text{for } R \geq S \qquad (7)$$

using rain depth $R$ and runoff depth, $V/(F_1 + F_2)$ = runoff volume/paved area. $S$ is the initial loss from wetting and depression storage and $\phi$ is a runoff volume coefficient defined relative to $F_1 + F_2$, and with consideration of $S$ as given by Eq. (7).

Only the single rain-runoff events within the period April 1-November 30 are used in order to exclude misinterpretations from snow and snow melt. Since all rain depths $R < S$ must be excluded in the regression, $A$ and $\phi$ were computed iteratively according to the following steps:

1) Make a guess $S_o$ of $S$ and reject all events with $R < S_o$.
2) Compute $\phi$ and $S$ by linear regression.
3) Put $S_o = S$ and repeat steps 1 and 2 until $S$-$S_o$ < convergence criteria (*eg.* 0,1 mm).

As an example Fig. 4 shows all single events (in 3 depth resolutions) and the regression line for CV.

The standard deviation

$$u = \left( \sum_{j=1}^{p} \frac{(V_j/(F_1+F_2)-\Phi(R_j-S))^2}{p-1} \right)^{\frac{1}{2}} \qquad (8)$$

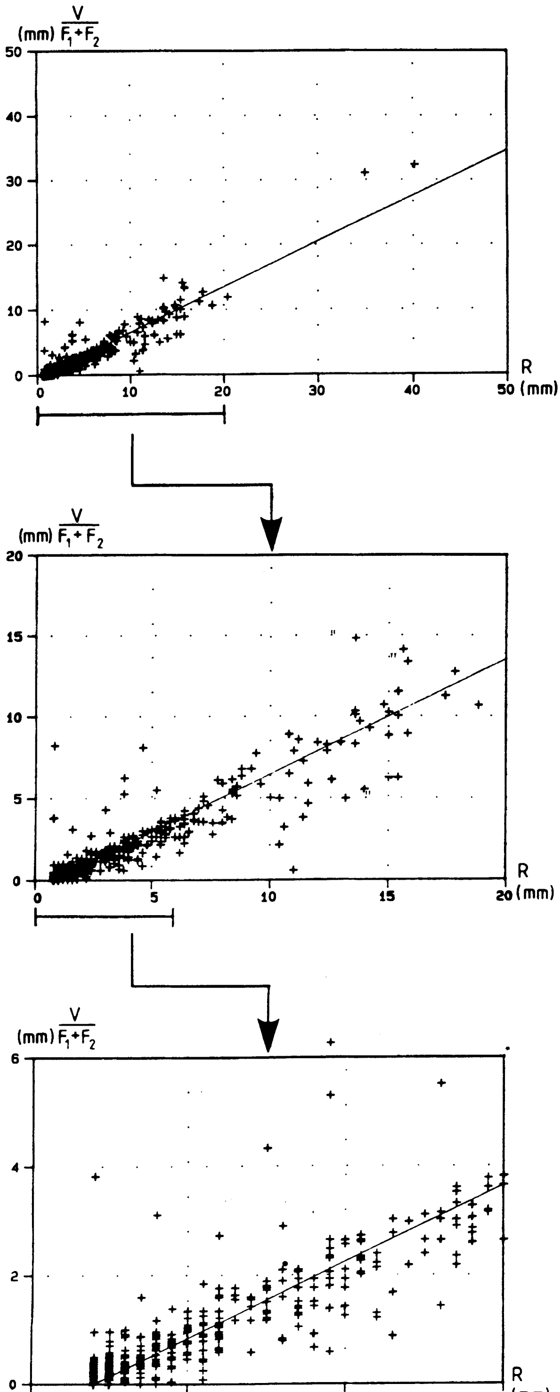


Fig. 4.
Linear regression between runoff $V/(F_1+F_2)$ and rain $R$ for CV.

is used as the goodness of fit, where $p$ is the number of single events with measured rain depth $R_j \geqslant S$ and $V_j$ is measured runoff volume.

Values of $\phi$, $S$ and $u$ appear in Table 4.

The lower $\phi$-values for EB and NV are possibly due to the relatively old pavement of these catchments (EB is from approx. 1940 and NV is from approx. 1900). The pavements, which here are considered impervious ($F_1$ in Table 1), can include cracks from traffic load and freezing through several decades.

The relatively high $\phi$-value for BB originates from 1.38 ha of highway asphaltic pavement from approx. 1970 (out of $F_1$ = 1.51 ha). This specific pavement was found to have a runoff coefficient of 0.98 by Jacobsen (1980).

The $u$ value for VP is significantly higher than $u$ for the other 5 catchments. This is due to the large green areas which contribute significantly to runoff from the most heavy rainfalls.

Table 4 – Runoff coefficient $\Phi$ initial loss $S$ and standard deviation $u$ from the linear regression model $V/(F_1+F_2) \equiv \Phi\ (R\text{-}S)$

| Catchment | Number of events $p(R \geqslant S)$ | Runoff coeff. $\Phi$ | Initial loss $S$ (mm) | Standard dev. $u$ (mm) |
|---|---|---|---|---|
| CV | 445 | 0.70 | 0.80 | 1.24 |
| MP | 507 | 0.70 | 0.48 | 1.24 |
| VP | 363 | 0.73 | 0.87 | 2.57 |
| EB | 362 | 0.61 | 0.92 | 1.35 |
| NV | 376 | 0.62 | 0.71 | 1.20 |
| BB | 254 | 0.84 | 0.70 | 0.90 |

## Continuous Hydrologic Model for Semipervious Areas

The simple linear regression in Eq. (7) is based on the concept that the runoff depth depends only on the rain depth $R$. In reality the runoff from semipervious and pervious areas is a function of several parameters such as the infiltration capacity and the intensity and duration of the individual rain. The infiltration capacity itself is a function of evaporation during the dry weather periods.

This section describes briefly the development and calibration of a continuous 10-parameter rain-runoff model for semipervious areas (a hydrologic model for both rain- and dry weather periods) paying attention to the processes just mentioned. Details may be seen in Jensen *et al.* (1985).

Fig. 5 is a conceptual illustration of the semipervious surfaces composed of impervious flagstones, with area $(1\text{-}b_2)F_2$, and cracks, with area $b_2F_2$, where infiltration takes place.

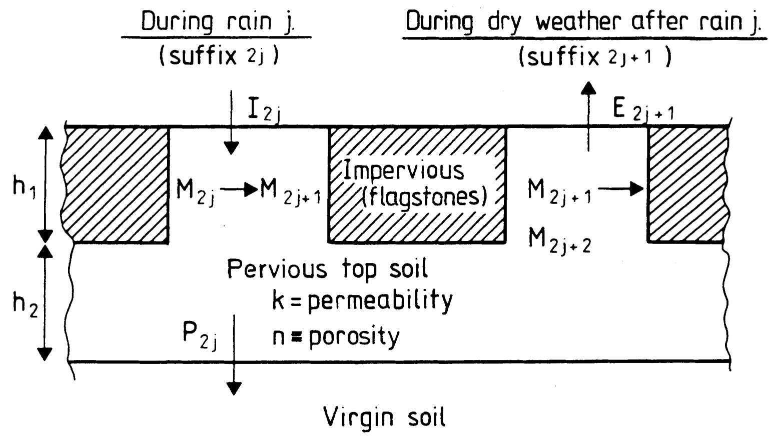


Fig. 5. Conceptual illustration of water balance in a semipervious pavement with cracks (exaggerated) separating the impervious flagstones.

During rain (suffix $2j$ where $j$ is the rain number), the initial loss $S=S_2$ will be retained on $F_2$ within a small duration (see Fig. 6). Hereafter the cracks are exposed to a rain with intensity $i_{2j}/b_2$, where $i_{2j}$ is the mean intensity. The factor $1/b_2$ corresponds to instantaneous runoff from the impervious flagstones to the separating cracks. The degree of saturation $a_{2j}$ within the top soil layer is defined by

$$M_{2j} = (b_2 h_1 + h_2) n a_{2j} = h_3 n a_{2j} \tag{9}$$

where $h_1$, $h_2$ and $h_3$ describes geometry (Fig. 5) and $n$ is porosity. The water content $M_3 = h_3 n a_3$, where $a_3$ is the field capacity, gives the upper limit of $M_{2j}$. For the smaller rains $M_{2j}$ increases with infiltration $I_{2j}$ to $M_{2j+1} = M_{2j} + I_{2j}$ ($\leq M_3$, Fig. 6 left) and no percolation occurs. However for more heavy rains the water content is restricted to $M_3$ and percolation ($P_{2j+2}$, Fig. 6 right) to the virgin soil takes place.

$I_{2j}$ is computed from the Hortonian infiltration capacity formula

$$f_c(t) = k + (f_{0,2j} - k) \exp(-ct) \tag{10}$$

where $k$ is approximately equal to the permeability of the top soil, $c$ is a decay constant, and $f_{0,2j}$ is the initial capacity, depending on $a_{2j}$. This dependence is taken from Jacobsen (1980) p. 145 (origin by Green and Ampt 1911)

$$f_{0,2j} = k(1 + \frac{h_0(1 - a_{2j})}{h_3 a_{2j}} \tag{11}$$

where $h_o$ is a depth constant for the top soil layer. Permeability $k$ is computed for each month corresponding to the monthly mean temperature.

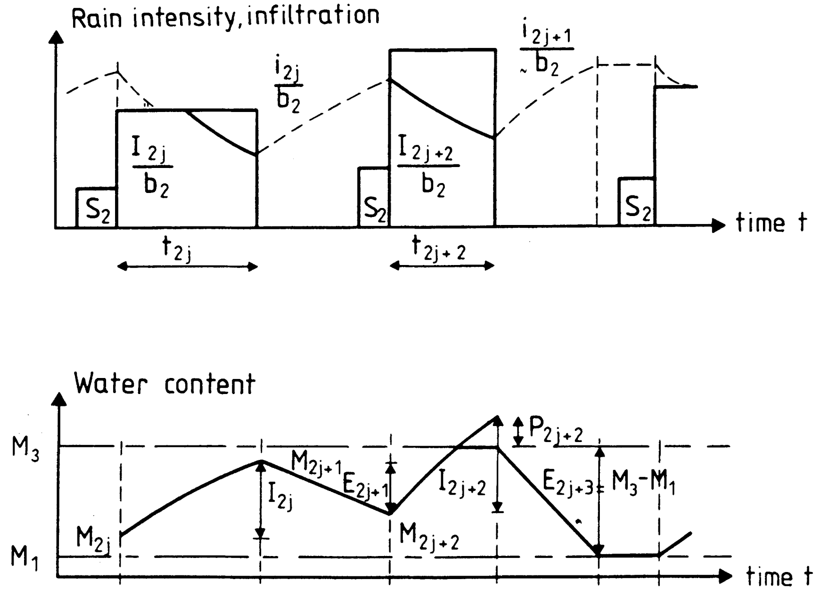


Fig. 6. Principle illustration of temporal distribution of water balance terms of a semipervious surface.

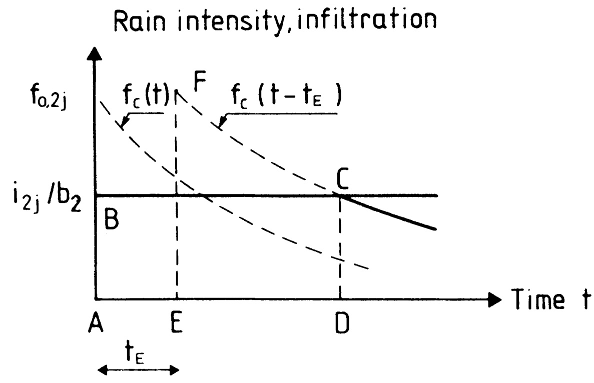


Fig. 7. Parallel displacement of infiltration capacity $f_c$ when $i_{2j}/b_2<f_{0,2j}$ (ABCD = CDEF) (cf. Tholin and Keifer 1960).

$I_{2j}$ is now found by integrating Eq. (11) after parallel displacement of $f_c(t)$ (Fig. 7), if $f_{o,2j} > i_{2j}/b_2$.

The infiltration parameters to be calibrated (and their expected values) are $b_2$ (order of magnitude 10 %), $h_3$ (order of magnitude 100 mm), $h_o$ (90 mm in Jacobsen 1980), $n$ (normally about 40 % for sand), $k_{10}$ (10°C; 10-100 $\mu$m/s for fine sand),

$c$ (0,6 × $10^{-3}$ $s^{-1}$ is applied in version of the computer program ILLUDAS), and $a_3$ (approximately 40 % in Jacobsen 1980).

During dry weather (suffix $2j + 1$) evaporation $E_{2j+1}$ decreases the water content. The intensity of actual evaporation $e$ is computed from

$$\frac{\text{actual evap.}}{\text{potential evap.}} \equiv \frac{e}{e_p} \equiv C_1 \equiv \text{constant} \tag{12}$$

(Høgh Jensen 1983). Potential evaporation has a remarkable daily variation and is almost zero at midnight (Jacobsen 1980, Appendix V). According to the fundamental theory of Penman (1948) $e_p$ depends on several climatic factors. These are, however, neglected, and $e_p$ is taken as a sinusoidal daily variation

$$e_p \equiv e_m (1 - \cos(2\pi \frac{t}{D})) \tag{13}$$

where $D \equiv 1$ day, $t \equiv 0$ at midnight and $e_m$ is the 12 monthly mean values of $e_p$ taken from Jacobsen (1980), p. 129. The possible depth of evaporation $E$ is thus computed by integrating Eq. (12). This $E$-value equals $E_{2j+1}$ when this means that $M_{2j+2} \geqslant M_1$ (Fig. 6 left), where the minimum water content $M_1 \equiv h_3 n a_1$ corresponds to the hygroscopic fixed degree of saturation $a_1$. Otherwise $E_{2j+1}$ is reduced so that $M_{2j+2} = M_1$ (Fig. 6 right).

The evaporation parameters to be calibrated (and their expected values) are the constants $C_1$ (17 % in Høgh Jensen 1983) and $a_1$ (order of magnitude 1 %).

The computed volume from impervious and semipervious areas, $F_1$ and $F_2$, is now given by

$$V_c = V_{1c} + V_{2c} = \Phi_1 F_1 (R-S) + F_2 (R-S-I_2) \tag{14}$$

where the initial loss $S$ is assumed identical for $F_1$ and $F_2$. The $S$-value is taken from Table 4.

Theoretically the runoff coefficient $\phi_1$ for impervious areas should be unity. However a detailed Swedish study by Falk and Niemczynowicz (1979) on 13 small asphaltic catchments have shown that some infiltration and/or gradual water storage in depressions takes place. They found $\phi_1 = 0.92$. Herein $\phi_1$ will be subject to calibration.

The total measured runoff volume is $V = V_1 + V_2 + V_3$, the contributions from the three types of areas. Except for heavy rains, which occur when the soil is already wet, $V_3$ will be small. Thus the present version of the model omits modelling of runoff from pervious areas $F_3$. However a principle is built into the model for detection of events, where runoff from $F_3$ is expected (see Jensen *et al.* 1985). Less than 5 % of the rainfalls showed runoff from $F_3$ according to this principle.

The 10 optimal parameter values of $b_2$, $h_3$, $h_o$, $n$, $k_{10}$, $c$, $a_3$, $C_1$, $a_1$, $\phi_1$ are defined as the set which gives the global minimum of the standard deviation

$$u = \frac{1}{F_1 + F_2} \left( \sum_{j=1}^{p} \frac{(V_j - V_{cj})^2}{p-1} \right)^{\frac{1}{2}} \tag{15}$$

where $V_j$ and $V_{cj}$ is measured and computed (Eq. (14)) runoff volume for rain No. $j$.

The calibration procedure is based on trial and error. The optimal values of $h_3$, $h_o$, $n$, $c$, $a_1$ and $a_3$ were practically identical for all 5 catchments (catchment BB is omitted since $F_2$ is almost zero), whereas optimal $\phi_1$, $b_2$, $k_{10}$ and $C_1$ did vary with catchment as seen in Table 5. In general the parameter values are in good agreement with the expected values mentioned above. However $u$ is not very sensitive to a change of parameter values. As an example Table 5 shows the small variations of $u$ for MP when $\phi_1$, $b_2$, $k_{10}$ and $C_1$ are subject to relatively large changes. This means that the optimal values are relatively uncertain.

It must be noted that the number of events $p$ in Table 5 is larger than $p$ in Table 4 due to omitting all rains with $R < S$ in Table 4.

When comparing $u$ in Table 5 with $u$ from the linear regression in Table 4, it can be seen that the continuous model gives a somewhat better fit to the measurements.

The figures $p$ (1+2) and $u$(1+2) are based on events where only runoff from $F_1$

Table 5 – Hydrologic parameters for impervious ($\Phi_1$) – and semipervious (all others) areas. For all 5 catchments is found: $h_3 \equiv 100$ mm; $h_0 = 110$ mm; $n = 40\%$; $c = 0.4\times10^{-3}s^{-1}$; $a_1 \equiv 1\%$; $a_3 \equiv 37.5\%$. Initial loss appear in Table 4.

| Catchment | Runoff coeff $\Phi_1$ (%) | Crack fract. $b_2$ (%) | Permeab. $k_{10}$ (μm/s) | Rel. evap. $C_1$ (%) | Number of Events $p$ | Number of Events $p(1+2)$ | Standard Deviation $u$ (mm) | Standard Deviation $u(1+2)$ (mm) |
|---|---|---|---|---|---|---|---|---|
| Optimal values (u(minimum)) | | | | | | | | |
| CV | 75 | 10 | 1.5 | 14 | 623 | 609 | 0.96 | 0.82 |
| MP | 80 | 11 | 1.7 | 28 | 656 | 621 | 1.06 | 0.96 |
| VP | 80 | 12 | 1.5 | 34 | 592 | 569 | 1.94 | 1.14 |
| EB | 75 | 10 | 8.0 | 17 | 626 | 616 | 1.05 | 0.63 |
| NV | 77 | 10 | 8.0 | 16 | 566 | – | 1.01 | – |
| Sensitivity analysis for MP | | | | | | | | |
| MP | 85 | 11 | 1.7 | 28 | 656 | 621 | 1.08 | 0.98 |
| MP | 75 | 11 | 1.7 | 28 | 656 | 621 | 1.06 | 0.96 |
| MP | 75 | 11 | 2.1 | 28 | 656 | 621 | 1.08 | 0.98 |
| MP | 75 | 11 | 1.1 | 28 | 656 | 621 | 1.07 | 0.97 |
| MP | 75 | 15 | 1.1 | 28 | 656 | 621 | 1.09 | 0.99 |
| MP | 75 | 7 | 1.1 | 28 | 656 | 621 | 1.09 | 0.99 |
| MP | 75 | 7 | 1.1 | 32 | 656 | 621 | 1.07 | 0.97 |
| MP | 75 | 7 | 1.1 | 24 | 656 | 621 | 1.08 | 0.98 |

and $F_2$ is expected, according to the principle mentioned above. For NV these computations have not been done because $F_3$ is very small. Since the model does not include computation of runoff from $F_3$, $u(1+2)$ is more justified for comparison with $u$ (Table 4). As can be seen the factor $u(1+2)/u$ (Table 4) varies between 44 % and 77 %. It should be mentioned that since rain and runoff measurements are subject to some inaccuracies, not considered herein, the above factor is even somewhat smaller.

Fig. 8 shows a comparison of the 50 largest measured runoff depths with computed values both from the continuous model and from the linear regression model, Eq. (7). These comparisons have not been carried out for catchments EB and NV. The continuous model predicts the measured runoff somewhat better than the linear regression for the most extreme events, say rank 1-5 (the bad agreement for VP is due to runoff from the large pervious area). For the more frequent events, however the two models are equally good. For most practical purposes, especially in applications where annual runoff is of concern, the linear regression model thus seems more attractive than the present continuous model.

## Long Term Water Balance for Semipervious Areas

By adding all the single event water balance terms in the water balance equations in the previous section a total water balance, valid for April-November can be set up for semipervious areas. This balance is based on computed values, except for the measured rain depth $R$.

$$\text{Rain-Initial loss - Runoff-Infiltration} = 0 \tag{16}$$

$$\text{Evaporation + Percolation - Infiltration} = 0 \tag{17}$$

These computations have been carried out for CV, MP and VP and as can be seen in Table 6, Eqs. (16) and (17) are satisfied. The table is commented as follows:

- Evaporation, which only refers to the process within the top soil layer of mean depth $b_2h_1+h_2$ (Fig. 5), is much larger for MP and VP due to the larger $C_1$-values (Eq. (12)) for these catchments.
- The initial loss is less than $pS_2$ (maximal initial loss) because several rains have depth $R<S_2$ (= maximum single event initial loss). Initial loss is believed to be that water depth which evaporates after each rain event.
- The mean runoff coefficient is 30-43 %. These figures compare rather well to the 44 % found by Jacobsen (1980) for a single inlet catchment, 682 m$^2$, of paving stones, and to 46 % referred in Statens Vejlaboratorium (1984) for the small, semipervious areas of catchment BB (Table 2).
- Percolation is almost the same for CV, MP and VP. This amount is an estimate of the ground-water recharge from semipervious areas.

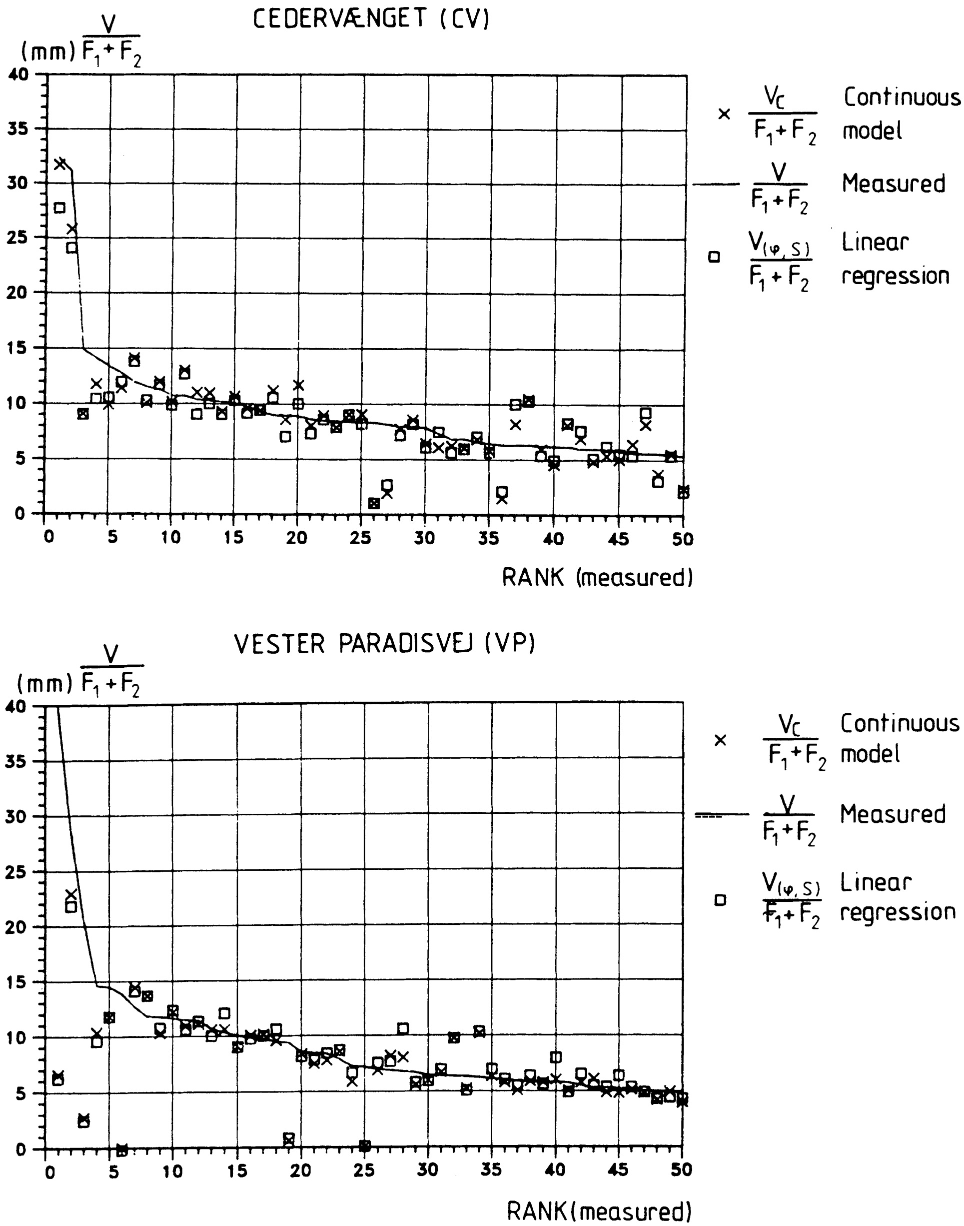


Fig. 8. Measured and computed runoff depths for the 50 single events with the largest runoff depths.

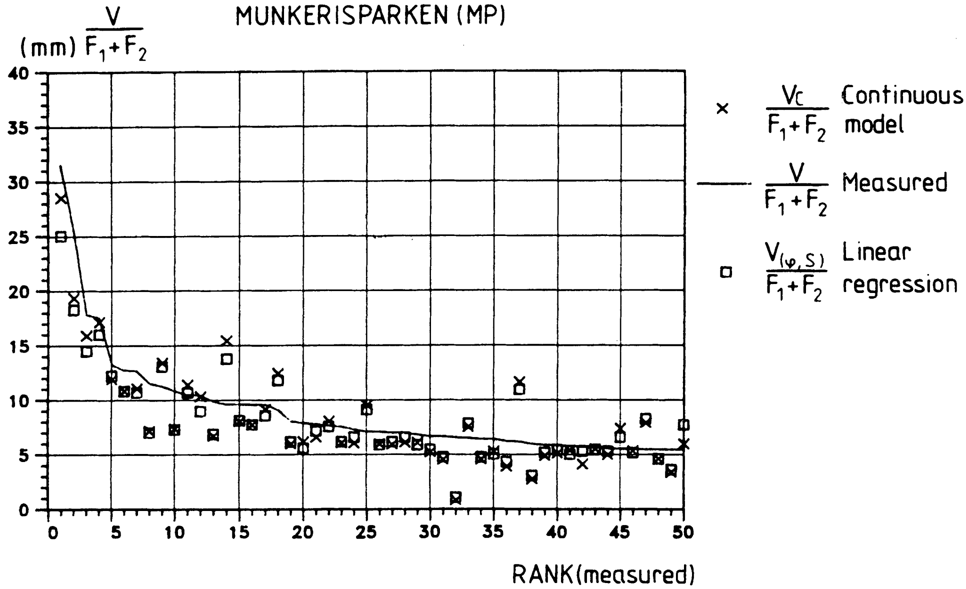


Fig. 8 continued

Table 6 – Total water balance, April-November, for semipervious surfaces.

| Catchment | CV | | MP | | VP | |
|---|---|---|---|---|---|---|
| Units | mm | % | mm | % | mm | % |
| Rain | 1,820 | 100.0 | 1,710 | 100.0 | 1,667 | 100.0 |
| – Initial loss | -437 | -24.0 | -303 | -17.7 | -437 | -26.2 |
| – Runoff | -787 | -43.2 | -627 | -36.7 | -495 | -29.7 |
| – Infiltration | -609 | -33.5 | -771 | -45.1 | -752 | -45.1 |
| Balance Eq. (16) | -13 | -0.7 | 9 | 0.5 | -17 | -1.0 |
| Evaporation | 281 | 15.4 | 497 | 29.1 | 493 | 29.6 |
| Percolation | 321 | 17.6 | 286 | 16.7 | 255 | 15.3 |
| Balance Eq. (17) | -7 | -0.4 | 12 | 0.7 | -4 | -0.2 |
| Events $p$ | 623 | | 656 | | 592 | |
| $S_2$ (mm) | 0.80 | | 0.48 | | 0.87 | |
| $b_2$ (%) | 10 | | 11 | | 12 | |
| $C_1$ (%) | 14 | | 28 | | 34 | |

## Conclusions

1) The continuous rain-runoff model, described herein, computes runoff from impervious – and semipervious areas $F_1$ and $F_2$ respectively. Runoff from $F_1$ is based on a runoff coefficient $\phi_1$ and initial loss $S$. Runoff from $F_2$ is computed as rainfall excess from block rains. Infiltration and percolation during rain and evaporation during dry weather involves 10 geometric-hydrologic parameters subject to calibration.
2) The continuous model is calibrated for each of 5 catchments, each having approximately 4 years of rain-runoff measurements. Only data from Apr. to Nov. has been used to avoid snow problems. The optimal values of the calibrated parameters agree well with similar values found elsewhere.
3) The standard deviation from the continuous model lies between 44 and 77 % of that from the linear regression model (rain depth versus runoff depth). This lower standard deviation is to some extent due to a better runoff prediction from the continuous model for rainfalls with extremely large runoff depth. When such events are of concern (*eg*. flooding), the application of the continuous model (possibly in an improved version) may be justified. However for more frequent events or annual runoff computations the linear regression model is adequate.
4) The continuous model estimates the percolation from semipervious surfaces to approx. 16 % of the total rain depth, April-November. The corresponding runoff coefficients lie between 30 and 43 %, in good agreement with values found elsewhere.
5) The intensity – duration frequency curves have shown variations up to approximately 20 % between catchments situated less than 15 km from each other for return periods 1/5 and 1/2 yr. These variations are considered mainly as spatial variability, and not only a consequence of the approximately 4 yr. period of record. The shape of the curves agrees with those based on long records (40 yr).
6) The peak discharge as a function of return period is compared with the corresponding rain intensity statistics. The discharge curve is mostly parallel to the rain curve, or has a slightly greater slope. This corresponds, respectively, to a constant or to a slight increase with return period for the peak runoff coefficient.

## Acknowledgement

The author is highly indebted to Dr. and Mrs. A. N. Neergaard Foundation for financial support to prepare the present paper.

## References

Falk, J., and Niemczynowicz, J. (1979) Modelling of runoff from impermeable surfaces, Dept of Water Resources Engineering, Univ. of Lund, Sweden, Rep. No. 3024.

Green, W.H., and Ampt, G.A. (1911) Studies on Soil Physics, 1. The Flow of Air and Water through Soils, *J. Agric. Sci., Vol. 4, No. 1,* 24 p.

Hansen, K.Å., and Kildebro, S. (1985) Regn og afstrømning (in Danish: Rain and Runoff), Dept. of Environmental Engineering, Technical Univ. of Denmark, 126 p., Examination Project.

Høgh Jensen, K. (1983) Simulation of water flow in the unsaturated zone including the root zone, Inst. of Hydrodynamics and Hydraulic Engineering, Technical Univ. of Denmark, Series paper No. 33.

Jacobsen, P. (1980) Urban Surface Runoff Simulation. Ph.D.Thesis, Dept. of Environmental Engineering, Technical Univ. of Denmark, Rep. 80-51, Vol. 1, 230 p.

Jensen, M., Strårup, J., Sørensen, B.E., and Jacobsen, C. (1985) Regnafstrømning i Mølleåsystemet, Bearbejdning af regn- og afstrømningsmålinger 1979-1983 (in Danish: Rain-runoff in the Mølleåsystem, Interpretation of measurements 1979-1983), Dept. of Environmental Engineering, Technical University of Denmark, 94 p.

Johansen, N.B., Dahi, E., Harremoes, P., Jensen, M., and Petersen, S. (1978-1981) Regnafstrømning i Mølleåsystemet (in Danish: Rain-Runoff in the Mølleåsystem), Dept. of Environmental Engineering, Technical University of Denmark, collective report and Vol. 1-6.

Johansen, N.B. (1985) Discharge to Receiving Waters from Sewer Systems during Rain. Ph.D.Thesis, Dept. of Environmental Engineering, Technical University of Denmark, 287 p.

Larsen, O. (1979) Sammenhørende målinger af nedbør og afstrømning fra befæstede arealer Emdrup Banke og Nannasgade-Vølundsgade. (In Danish: Connected measurements of rain and runoff from paved areas of Emdrup Banke and Nannasgade-Vølundsgade), Spildevandskomiteen, Dansk Ingeniørforening.

Penman, H.L. (1948) Natural evaporation from open water, bare soil and grass, Proc.Roy.-Soc., A 193, 120 p.

Spildevandskomitéen, DIF (the Waste Water Commity within The Danish Society of M.Sc. Engineers) (1977) Bestemmelse af regnrækker (in Danish: Derivation of Intensity-Duration-Frequency Curves), Paper No. 16.

Statens Vejlaboratorium (Road Laboratory of Denmark) (1984) Regn- og afstrømningsmålinger fra Bispeengsbuen og Holbækmotorvejen (in Danish: Rain – an Runoff Measurements from Bispeengsbuen and the Motorway of Holbæk), Report No. 164.

Tholin, A.L., and Keifer, C.J. (1960) The hydrology of urban runoff, Transactions of the American Society of Civil Engineers, Vol. 125, pp. 1308-1379.

First received: 25 April, 1989
Revised version received: 15 November, 1989
Accepted: 22 November, 1989

**Address:**
Danish Isotope Centre,
Academy of Technical Sciences,
Skelbækgade 2,
DK-1717 Copenhagen,
Denmark.